NWTによるKolmogorov(1962)相似仮説の検証(渦度場の幾何学的構造と乱流統計)

AUTHOR(S):

Hosokawa, Iwao; Oide, Shin-ichi; Yamamoto, Kiyoshi

CITATION:

Hosokawa, Iwao ...[et al]. NWTによるKolmogorov(1962)相似仮説の検証(渦度場の幾何学的構造と乱流統計). 数理解析研究所講究録 1996, 972: 97-108

ISSUE DATE:

1996-11

URL:

http://hdl.handle.net/2433/60723

数理解析研究所講究録
972巻 1996年 97-108

NWTによるKolmogorov (1962)相似仮説の検証

電通大　細川　巖、生出伸一
航空技研　山本稀義

Non-Trivial Difference in Effect between the True Dissipation Rate and Its 1D Surrogate in Isotropic Turbulence

Iwao Hosokawa and Shin-ichi Oide
University of Electro-Communications, Chofu, Tokyo 182, Japan

Kiyoshi Yamamoto
National Aerospace Laboratory, Chofu, Tokyo 182, Japan

While the one-dimensional surrogate of energy dissipation rate has often been used in place of the true one in many researches in context to the refined similarity hypothsis of Kolmogorov and the multifractal nature of isotropic turbulence, it is reported here, as a result of direct numerical simulation, that there is a fundamental difference between the two results which the surrogate and the true one bring forth. The conditional and unconditional probability density of the Kolmogorov variable in terms of the true one are never bimodal but always nearly Gaussian. The multifractal nature of dissipation and possible fractional Brownian motion of velocity in turbulence often discussed are substantially affected by this fact.

Many people who investigate isotropic turbulence experimentally have been using the so-called pseudo-dissipation rate $\varepsilon' = 15\nu(\partial u/\partial x)^2$ (ν: kinematic viscosity, $\partial u/\partial x$: longitudinal velocity gradient), that is the one-dimensional (1D) surrogate of energy dissipation rate ε in isotropic turbulence in place of ε itself, simply because it is hard to measure all the simultaneous components of strain tensor. In most cases, discussions of intermittency exponents have been based on observations of the surrogate ε' (with invoking the Taylor hypothesis). In particular, it is to be remarked that several current important ideas on the fine structure of turbulence, such as the multifractal distribution of dissipation in space [1], the bimodality of conditional probability density functions (PDF) for a small scale range [2] of the Kolmogorov variable in the refined similarity hypothesis (RSH) [3], and the fractional Brownian motion (FBM) of velocity increment [4], have been established on the basis of the knowledge obtained from observation of the surrogate ε'.

However, the true ε may give a different knowledge leading to different ideas. Such a possibility was already pointed out by some people [5-8]. Here we present the comparison of the results obtained by using ε and that by ε' from the data sets of direct numerical simulation (DNS) of two decaying isotropic turbulences at the fully-developed state with $R_\lambda \sim 100$ [9] and ~ 160 [10] (R_λ: Taylor-scale Reynolds number) on a 128^3 and a 512^3 grid, respectively. (The method of calculation on the former grid was described in [11]; it is characteristic in using the decomposed solenoidal field of velocity and simply employing the Runge-Kutta-Gill scheme for time-integration, and it is the same on the latter grid, too, but the calculation was performed by the NAL numerical wind tunnel, a distributed memory-parallel computer with 128 vector-type processor elements, which achieved 113.8 GFLOPS for FFT and 90.3 GFLOPS for this turbulence scheme, gifting the operation team the 1994 Gordon Bell Prize of IEEE Computer Society.)

First we show in Fig. 1(a) the unconditional PDF's of the Kolmogorov variable v defined by RSH for various fixed scales r:

$$\Delta u_r = v(r\varepsilon_r)^{1/3}, \qquad (1)$$

where Δu_r is longitudinal velocity increment across distance r, and ε_r is ε averaged over a domain of scale r; we take the domain as the cube with side-length r between the centers of opposite faces of which the Δu_r is measured. v is normalized by its root mean square. They are skewed somewhat (at most, -0.3) but very similar to Gaussian, even though slightly depending on r. In contrast, we can see in Fig. 1(b) those for the surrogate dissipation using ε'_r in place of ε_r; in this case ε'_r is defined as the average of ε' over a line of

length r across which Δu_r is measured. Apparently, they are bimodal for small r and gradually approach to Gaussian as r increases. These data in Fig. 1 come from the computation for $R_\lambda \sim 160$, and 9 cases of r/η are plotted ranging from 0.580 to 149 (η: Kolmogorov length), so that the inertial range covers r/η = 4.64, 9.28 and 18.6. The bimodality seen here seems to reflect that of the conditinal PDF's of v for the surrogate dissipation, which were depicted in detail by Stolovitzky et al. [2] based on the experimental observation of real turbulence in an atmospheric surface layer with $R_\lambda \sim$ 1500 and 2000. Since we are interested in the existence or non-existence of bimodality, we show the conditinal PDF's of v for ε_r and ε'_r only for a small r (r/η = 1.16) in Fig. 1(c) and (d). It is evident that there is no bimodality found in the conditional PDF's of v for ε_r even for such a small r for any $(r\varepsilon_r)^{1/3}$ and the PDF hardly depends on $(r\varepsilon_r)^{1/3}$, while that for ε'_r is clearly bimodal and strongly depends on $(r\varepsilon'_r)^{1/3}$; the more bimodal for the larger $(r\varepsilon'_r)^{1/3}$. Every lines are drawn for a value zone of $(r\varepsilon_r)^{1/3}$ or $(r\varepsilon'_r)^{1/3}$ which is one of the octad made by dividing the whole zone between the maximum and minimum of $(r\varepsilon_r)^{1/3}$ or $(r\varepsilon'_r)^{1/3}$ into 8, only when each zone has a sufficient number of data points to draw a line. Ruggedness of lines means that the data number is relatively small, and it happens usually when $(r\varepsilon_r)^{1/3}$ or $(r\varepsilon'_r)^{1/3}$ is large but also when it is very small for large r. In Fig. 1(d), however, we notice that the transition pattern of the conditional PDF with $(r\varepsilon'_r)^{1/3}$ is reverse to what was presented in [2] but resembles a *persistent case* of the process treated in [4]; as $(r\varepsilon'_r)^{1/3}$ increases, the line moves from outside to inside. We show the same comparison for r/η = 4.64 and 9.28 in Fig. 2. Fig. 2(a) and (c) identifies the tendency which appeared in Fig. 1(c) and the more Gaussianization of PDF holding a skewness. In Fig. 2(b) we can see that the conditional PDF for ε'_r still keeps bimodality for smaller $(r\varepsilon'_r)^{1/3}$ but the transition pattern is now similar to that in [2], resembling an *anti-persistent case* [4]. Fig. 2(d) has the same trend, but the conditional PDF's for larger $(r\varepsilon'_r)^{1/3}$ approach to Gaussian. For larger r we have made sure that the conditional PDF for the true dissipation approaches to Gaussian in a simple way, while that for the surrogate does so considerably depending on $(r\varepsilon'_r)^{1/3}$ even in the inertial range (faster for larger $(r\varepsilon'_r)^{1/3}$) just as is presented in [2]. (We here note that no Taylor hypothesis was invoked in our calculation and this may cause such a small difference in the conditional PDF for the surrogate between our result and [2] as we have just seen; but also other reasons such as a difference of resolution may come in to cause it.)

Thus, it is natural to conclude that the bimodality is peculiar to the PDF of v for the surrogate dissipation, and that the PDF of v for the true

dissipation may be assumed as nearly Gaussian for a wide range of r and is hardly conditioned by $(r\varepsilon_r)^{1/3}$, but slightly dependent on r [12]. For reference, we show the skewness and kurtosis of the unconditinal PDF of the true dissipation against r/η in Fig. 3, whence we see an appreciable dependence of the kurtosis on r in the inertial range (inserted by arrows). By the way, we note that the ensemble average of unnomralized v^3, say $\langle v^3 \rangle$, in the inertial range is just around -1, which roughly approximates -4/5 in the Kolmogorov theory [13]:

$$\langle \Delta u_r^3 \rangle = -4/5\ r\langle \varepsilon_r \rangle. \qquad (2)$$

(Note that v is almost independent of $(r\varepsilon_r)^{1/3}$ for the true dissipation.) This may indicate a limit of simulation of the ideal state ($R_\lambda \to \infty$) which can be achieved by our DNS turbulence with a rather low R_λ. On the other hand, we have got about 2.7 as $\langle v^2 \rangle$ in the inertial range, which consistently gives nearly the Kolmogorov constant C_K for our turbulence, 2.1, again the same as in [11], by dividing by $55/27\Gamma(1/3)$ [14]; intermittency effect for $\langle \varepsilon_r^{2/3} \rangle$ is negligible here. (This rather high value of C_K is common to other current DNS's of turbulence. We verified that, as both $\langle v^3 \rangle$ and $\langle v^2 \rangle$ depend on r in such a way that the magnitudes of them decrease outside the inertial range, the averages of them over a wider range of r get closer to the ideal values.)

Next, we may be tempted to imagine the FBM of velocity with Hurst number 1/3 from the form of (1). Indeed, Stolovitzky and Sreenivasan [15] succeeded in deriving theoretically the conditional PDF of v from such a general point of view by utilizing a special analytical relationship of Δu_r and $r\varepsilon'_r$ through the quantity $\partial u/\partial x$ with some assumptions. That is bimodal for small r and approaches to Gaussian for large r in rather excellent agreement with their experimental observation, but without any skewness. However, since the PDF of v is not really bimodal as we have seen above, their theory is not fit to reality. Nevertheless, there remains a question whether turbulent velocity makes actually an FBM. Then we have investigated this point by observing the correlation function which was presented by Feder [16] to judge the existence of FBM:

$$C(r) = \langle \Delta u_r\, \Delta u_{-r} \rangle / \langle \Delta u_r^2 \rangle. \qquad (3)$$

Only if it is a constant equal to $1 - 2^{2H-1}$, the motion can be judged as the FBM with Hurst number H. Our results of C(r) for $R_\lambda \sim 100$ and 160 are shown in Fig. 4. They never reveal any constancy even in the inertial range (inserted by arrows) but gradually increase with r/L (L: largest scale in DNS) far over the constant line corresponding to H = 1/3. Therefore, it is hard to think that the form of RSH leads to FBM naturally. It may be too naive to expect an FBM of velocity only by the form of (1), since we have another stochastic variable

ε_r than the nealy Gaussain random variable v. We note that C(r) = -1 at r = 0 as it should if u_r is analytic, and that C(r) = 1 at r = L/2 is due to the periodic boundary condition so that the behavior beyond r = L/4 would be unrealistic. Zhu and Antonia traced the behavior of C(r) for the turbulence in an atmospheric surface layer with $R_\lambda \sim 7200$, but a clear constancy to indicate H = 1/3 was not obtained [17]. We may expect experimentalists to re-examine C(r) for other cases with a sufficient amount of data to avoid a scattered result. This is a fundamentally interesting problem. By the way, we may point out that the persistent character of the pattern in Fig. 1(d) reasonably corresponds to the fact that C(r) in Fig. 4 is negative for $r/\eta = 1.16$ so that H > 1/2 if the process treated in [15] would be supposed to exist in a local sense, while the anti-persistent character in Fig. 2 (b) and (d) corresponds to the fact that C(r) is positive for $r/\eta = 4.64$ and 9.28 so that H < 1/2. These facts appear to reconfirm well the trend of the theoretical PDF with an arbitrary H deduced in [15].

In Fig. 5, we compare the generalized dimensions D(q) obtained for the surrogate measure with those for the true dissipation measure. Here we understand that the former gives a multifractal in the 1D space (or a 1D cut of the 3D space). So let us distinguish it as $D(q)^{(1)}$ from D(q) in the 3D space. Since we have many lines of length L in the DNS box of turbulence, we can get many $D(q)^{(1)}$'s calculated in every line by the box counting method [18]. Just as in the experiment by Meneveau and Sreenivasan [19], these $D(q)^{(1)}$'s scatter in a wide range. Then we plot the averaged $D(q)^{(1)}$ over all of them (128^2 $D(q)^{(1)}$'s for $R_\lambda \sim 100$) by closed diamonds in the Figure and compare it with the p model [19] indicated by a dashed line. Note that we set $D(q) = D(q)^{(1)} + 2$ as the 3D version of the multifractal [20]. Hence we may judge that our DNS supports the p model very well, only if the surrogate is treated in the 1D space. On the other hand, the D(q)'s for the true dissipation (by the 3D box counting method) are plotted by closed circles and crosses for $R_\lambda \sim 160$ and 100, respectively. These are close to each other, suggesting the robustness of D(q) of the multifractal of dissipation measure in the 3D space. Thus, there is a non-trivial difference between D(q) for the surrogate and that for the true dissipation. Only for |q| < 3 both are coincident. The trinomial generalized Cantor set model [21] (contrived to improve the 3D binomial Cantor set model [22] and indicated by open triangles here) with intermittency exponents:

$$\mu(q) = \log_A(\nu_1 B^q + \nu_2 M^q + \nu_3 C^q), \qquad (3)$$

where A = 1.45214, B = 1.32284, M = 1.04693, C = 0.62732, $\nu_1 = 0.326569$, $\nu_2 = 0.346863$ and $\nu_3 = 0.326569$, is in excellent agreement with the DNS in the

entire region. (Note that $D(q) = -\mu(q)/(q - 1) + 3.$) We add in the Figure the She-Leveque model [23] which is not simply phenomenological but based on some concepts on the dynamics and has intermittency exponents:

$$\mu(q) = 2q/3 - 2[1 - (2/3)^q]. \quad (4)$$

This model, indicated by a solid line, is very close to our DNS and the trinomial generalized Cantor set model only for $q \geq 0$. Thus we may understand that the p model extracted from $D(q)^{(1)}$ plays a good role in treating a nature of turbulence relevant to low-order moments of Δu_r in the inertial range, but otherwise it had better be replaced by a better model.

In conclusion, we disclosed a non-trivial difference in effect between the true dissipation rate and its 1D surrogate in isotropic turbulence, by treating the PDF of v, the possibility of FBM of longitudinal velocity, and the multifractal nature of dissipation on the basis of our DNS data. Chen et al. [24] addressed no qualitative difference in result between both in the treatment of conditional average of $|\Delta u_r|$, but they did not analyze such detailed features as treated here. On the other hand, Wang et al. [25] found a large difference in some aspects related to RSH between both. Our result makes the detail and effect of the difference clear. Even though the R_λ reached by the DNS is still low as compared with that by experiment, the present result indicates a need to reconsider any induction only based on the knowledge from the 1D surrogate dissipation.

This work was in support of the Grant-in-Aid for Scientific Research from the Ministry of Education, Science and Culture of Japan

References

[1] C. Meneveau and K. R. Sreenivasan, Phys. Rev. Lett. **59**, 1424 (1987).

[2] G. Stolovitzky, P. Kailasnath, and K. R. Sreenivasan, Phys. Rev. Lett. **69**, 1178 (1992).

[3] A. N. Kolmogorov, J. Fluid Mech. **13**, 82 (1962).

[4] G. Stolovitzky and K. R. Sreenivasan, Rev. Mod. Phys. **66**, 229 (1994).

[5] R. Narasimha reports Roger and Moin's (1987) result in *Turbulence at the Cross Roads*, ed. J. L. Lumley (Springer, Berlin, 1990) p. 13.

[6] A. Tsinober, E. Kit, and T. Dracos, in *Advances in Turbulence 3, ed. A. V. Johansson and P. H. Alfredsson* (Springer, Heidelberg, 1991) p. 514.

[7] I. Hosokawa, J. Phys. Soc. Jpn. **64**, 3141 (1995).

[8] S. T. Thoroddsen, Phys. Fluids **7**, 691 (1995).

[9] I. Hosokawa and K. Yamamoto, J. Phys. Soc. Jpn **59**, 401 (1990); Phys. Fluids A 2, 889 (1990); in *Turbulence and Coherent Structures,* ed. O. Metais & M. Lesieur (Kluwer, Dordrecht, 1991), p. 177.

[10] K. Yamamoto, I. Hosokawa, and K. Sakai, Res. Inst. Math. Sci. Rep. (Kokyuuroku) **892** (1995) 217; K. Yamamoto, Nagare (J. Japan Soc. Fluid Mech.) **14** (1995) 353.

[11] K. Yamamoto and I. Hosokawa, J. Phys. Soc. Jpn. **57**, 1532 (1988).

[12] This validates the treatment of the PDF and scaling nature of velocity increment in I. Hosokawa, J. Phys. Soc. Jpn. **62**, 3792 (1993); Phys. Rev. E 51, 781 (1995); Fluid Dyn. Res. **15**, 337 (1995); J. Phys. Soc. Jpn. **64**, 3141 (1995).

[13] A. N. Kolmogorov, Dokl. Acad. Nauk USSR **31**, 538 (1941).

[14] A. S. Monin and A. M. Yaglom, *Statistical Fluid Mechanics,* Vol. 2 (MIT, 1975), p. 355.

[15] G. Stolovitzky and K. R. Sreenivasan, Rev. Mod. Phys. **66**, 229 (1994).

[16] J. Feder, Fractals (Plenum Press, New York, 1988), p. 170; the formula of C(t) there is erroneous by factor 2.

[17] Private communication.

[18] T. C. Halsey, M. H. Jensen, L. P. Kadanoff, I. Procaccia and B. I. Shraiman, Phys. Rev. A **33**, 1141 (1986).

[19] C. Menevearu and K. R. Sreenivasan, Nucl. Phys. B (Proc. Suppl.) **2**, 49 (1987).

[20] C. Menevearu and K. R. Sreenivasan, Phys. Rev. Lett. **59**, 1424 (1987).

[21] I. Hosokawa, S. Oide, and K. Yamamoto, J. Phys. Soc. Jpn., submitted.

[22] I. Hosokawa, Phys. Rev. Lett. **66**, 1054 (1991).

[23] Z.-S. She and E. Leveque, Phys. Rev. Lett. **72**, 336 (1994).

[24] S. Chen, G. D. Doolen, R. H. Kraichnan, and Z.-S. She, Phy. Fluids A **5**, 458 (1993).

[25] L.-P. Wang, S. Chen, J. G Brasseur, and J. C. Wyngaard, J. Fluid Mech., submitted.

Figure captions

Fig. 1 The unconditional PDF's of v for various r for (a) the true dissipation and (b) its 1D surrogate; r/η = 0.586, 1.16, 2.32, 4.64, 9.28, 18.6, 37.2, 74.3, 149; as r/η increases, the line moves to the outside. The conditional PDF's of v for r/η = 1.16 for several values of (c) $(r\varepsilon_r)^{1/3}$ and (d) $(r\varepsilon'_r)^{1/3}$; as $(r\varepsilon'_r)^{1/3}$ increases, the line moves to the inside. The dotted lines denote the standard normal PDF.

Fig. 2 The conditional PDF's of v for r/η = 4.64 for several values of (a) $(r\varepsilon_r)^{1/3}$ and (b) $(r\varepsilon'_r)^{1/3}$. The conditional PDF's of v for r/η = 9.28 for several values of (c) $(r\varepsilon_r)^{1/3}$ and (d) $(r\varepsilon'_r)^{1/3}$. As $(r\varepsilon'_r)^{1/3}$ increases, the line moves to the outside for both cases. The dotted lines denote the standard normal PDF.

Fig. 3 (a) Skewness and (b) kurtosis of PDF of v for the true dissipation against r/η for $R_\lambda \sim 160$ (solid line) and $R_\lambda \sim 100$ (dotted line). The inertial range of each case is indicated by the inserting arrows.

Fig. 4 Feder's correlation function of Δu_r for $R_\lambda \sim 160$ (solid line) and $R_\lambda \sim 100$ (dotted line), the inertial range of each case being indicated by the inserting arrows. Horizontal lines show the fractional Brownian motions with various Hurst numbers.

Fig. 5 Generalized dimensions D(q)'s for $R_\lambda \sim 160$ (closed circles), for $R_\lambda \sim 100$ (crosses), and for the trinomial generalized Cantor set model (open triangles). $D^{(1)}(q) + 2$ for the p model is indicated by a dashed line and the average $D^{(1)}(q) + 2$ for the 1D surrogate dissipation for $R_\lambda \sim 100$ by closed diamonds. The She-Leveque model is added by a solid line, which overlaps with closed circles, crosses, and open triangles for $q \geq 0$.

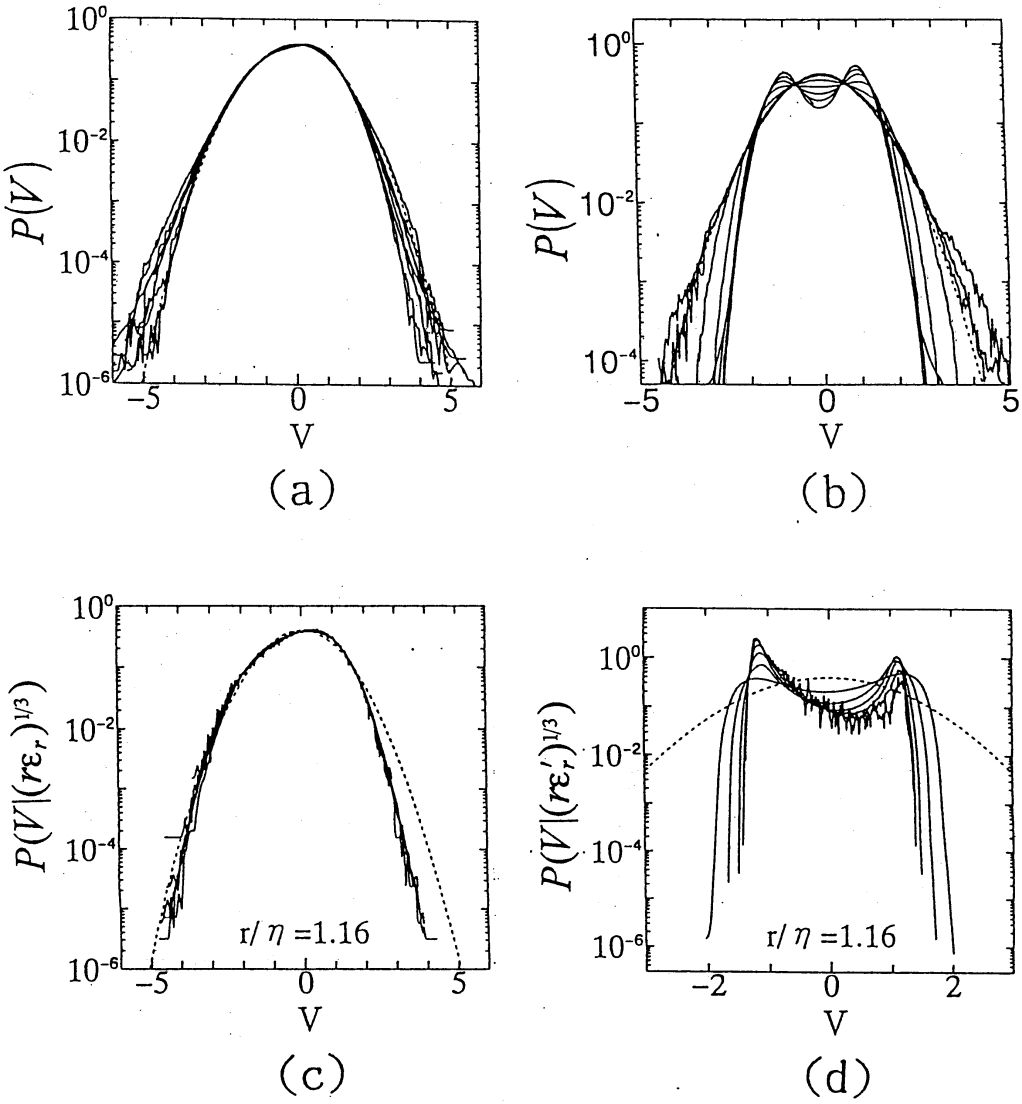
10^0
10^{-2}
10^{-4}
10^{-6}
$P(V)$
−5
0
5
V
(a)
10^0
10^{-2}
10^{-4}
$P(V)$
−5
0
5
V
(b)
10^0
10^{-2}
10^{-4}
10^{-6}
$P(V|(r\varepsilon_r)^{1/3})$
r/ η =1.16
−5
0
5
V
(c)
10^0
10^{-2}
10^{-4}
10^{-6}
$P(V|(r\varepsilon_r')^{1/3})$
r/ η =1.16
−2
0
2
V
(d)

Fig.1

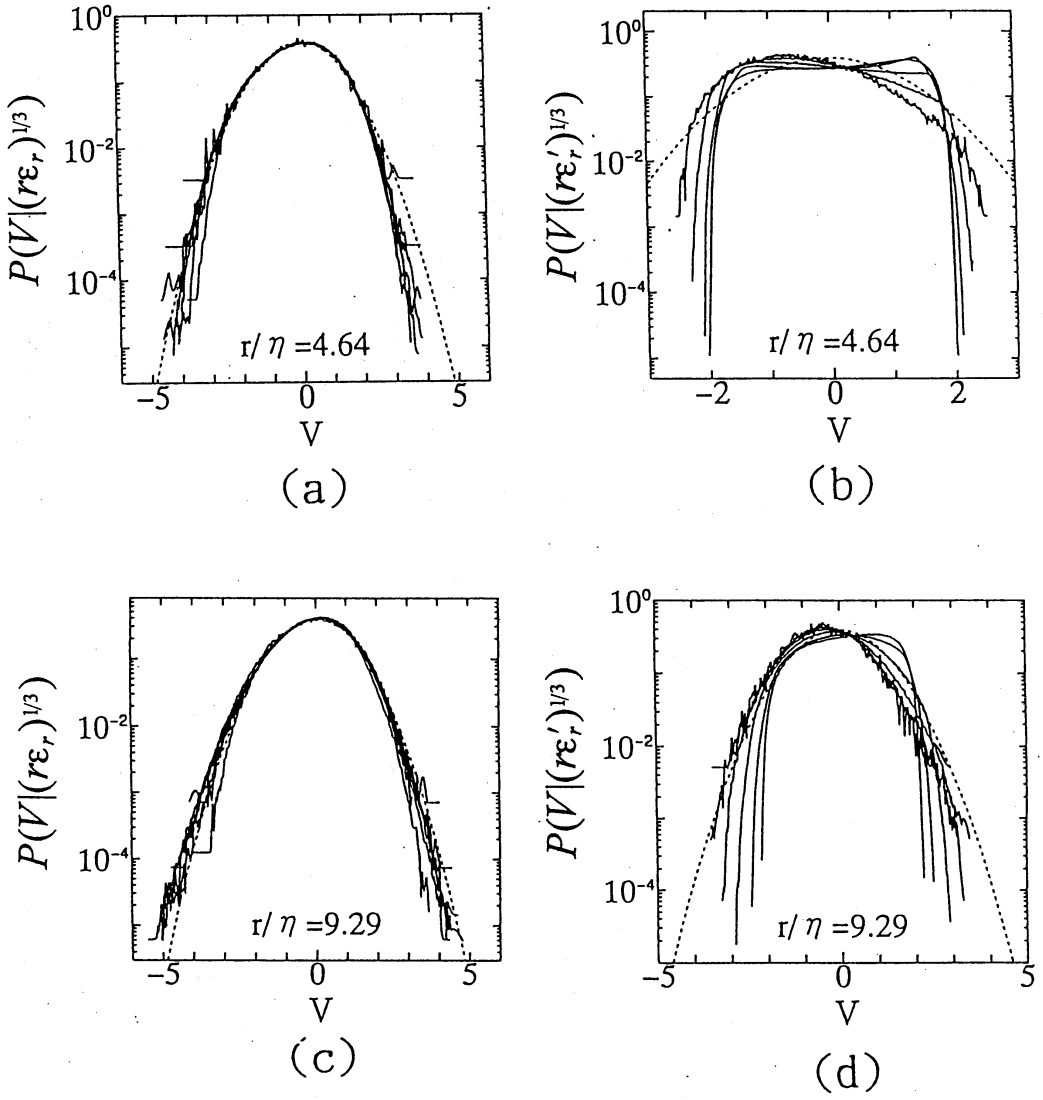
$P(V|(r\varepsilon_r)^{1/3})$
10^0
10^{-2}
10^{-4}
r/ η =4.64
−5
0
5
V
(a)
$P(V|(r\varepsilon_r')^{1/3})$
r/ η =4.64
−2
2
(b)
r/ η =9.29
(c)
r/ η =9.29
(d)

Fig.2

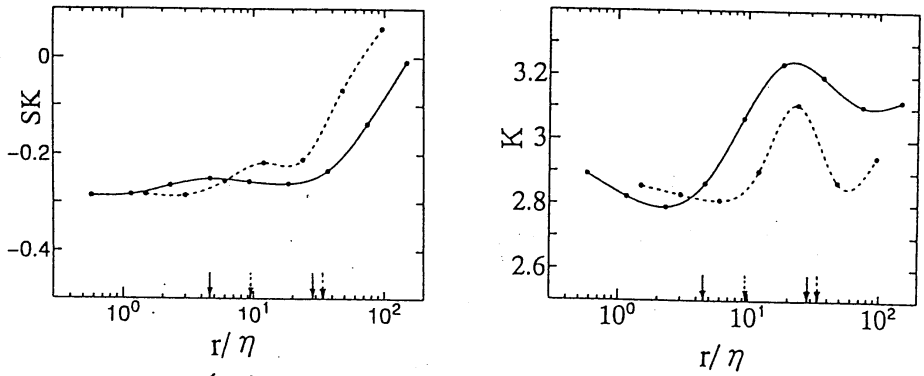
SK
0
-0.2
-0.4
10^0
10^1
10^2
r/ η
(a)
K
3.2
3
2.8
2.6
10^0
10^1
10^2
r/ η
(b)

Fig.3

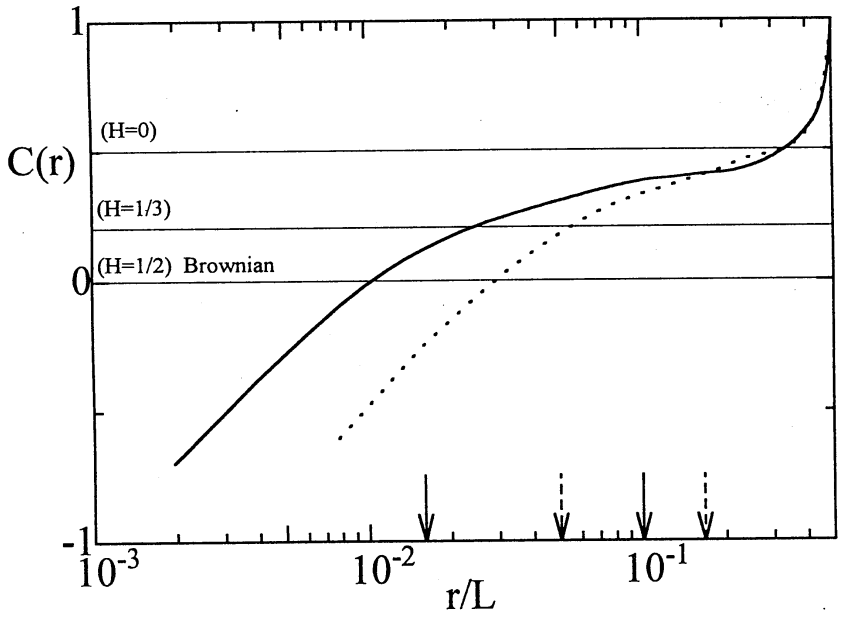
1
C(r)
(H=0)
(H=1/3)
0
(H=1/2) Brownian
-1
10^{-3}
10^{-2}
10^{-1}
r/L

Fig.4

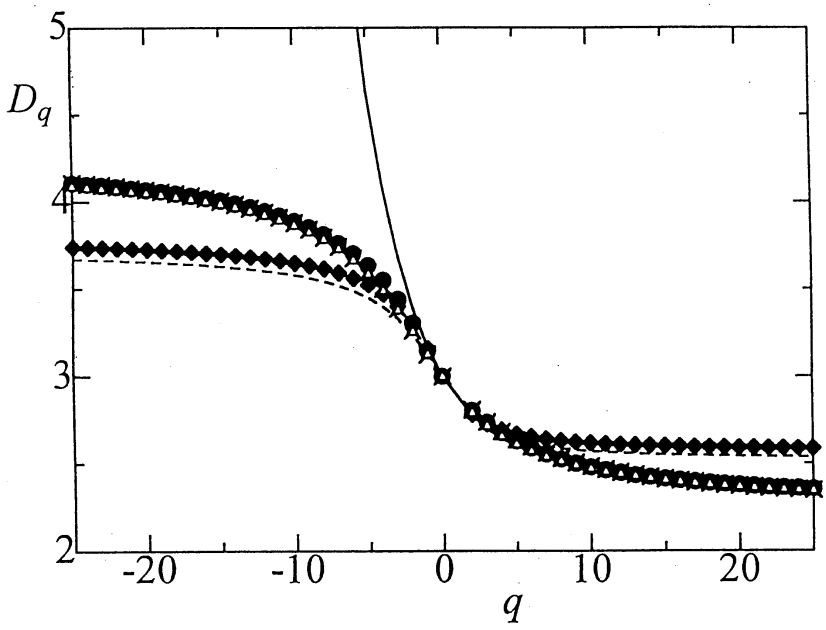

Fig.5